JOURNAL OF Materials CHEMISTRY

Preparation and characterization of a novel magnetic nano-adsorbent

Min-Hung Liao and Dong-Hwang Chen*

Department of Chemical Engineering, National Cheng Kung University, Tainan 701, Taiwan. E-mail: chendh@mail.ncku.edu.tw

Received 22nd July 2002, Accepted 16th October 2002
First published as an Advance Article on the web 5th November 2002

A novel magnetic nano-adsorbent has been developed using Fe_3O_4 nanoparticles (13.2 nm) as cores and polyacrylic acid (PAA) as ionic exchange groups. The Fe_3O_4 magnetic nanoparticles were prepared by co-precipitating Fe^{2+} and Fe^{3+} ions in an ammonia solution and treating under hydrothermal conditions. PAA was covalently bound onto the magnetic nanoparticles *via* carbodiimide activation. Transmission electron micrographs showed that the magnetic nanoparticles remained discrete and had no significant change in size after binding the PAA. The X-ray diffraction patterns indicated the magnetic nanoparticles were pure Fe_3O_4 with a spinel structure, and the binding of PAA did not result in a phase change. Magnetic measurement revealed the magnetic nanoparticles were superparamagnetic, and their saturation magnetization was reduced only slightly after PAA binding. Fourier transform infrared spectroscopy, thermogravimetric and differential thermal analyses, and X-ray photoelectron spectroscopy confirmed the binding of PAA to the magnetic nanoparticles, suggested a binding mechanism for the PAA, and revealed the maximum weight ratio of PAA bound to the magnetic nanoparticles was 0.12. In addition, the ionic exchange capacity of the resultant magnetic nano-adsorbents was estimated to be 1.64 mequiv g^{-1}, much higher than those of commercial ionic exchange resins. When the magnetic nano-adsorbents were used for the recovery of lysozyme, the adsorption/desorption of lysozyme was completed within 1 min due to the absence of pore-diffusion resistance. Also, the adsorption/desorption efficiency could reach almost 100% under appropriate conditions, and the recovered lysozyme retained 95% activity.

Introduction

During the past decade, an immense amount of work has been done on nanostructured materials because of their unusual physical and chemical properties owing to their extremely small size and large specific surface area.[1] Recently, considerable effort has been made on the surface modification of nanoparticles and the preparation of organic–inorganic nanocomposites. The combination of inorganic and organic (may be bioactive) components in a single particle at the nano-sized level has made accessible an immense area of new functional materials.[2–16]

Adsorption is a conventional but important separation process. It has been used widely in the chemical, biological, analytical, and environmental fields. In most cases, the adsorbents have diameters in the range of sub-micron to micron and have large internal porosities to ensure adequate surface area for adsorption. However, the diffusion limitations within the particles lead to decreases in the adsorption rate and the available capacity, particularly for macromolecules such as proteins and DNA. So, it is interesting and there is an incentive to develop a novel adsorbent with a large surface area for adsorption, a small diffusion resistance, and a high capacity for large solutes.

Nonporous nanoparticles may meet the above requirements. However, because nanoparticles are quite small, the adsorptive process may be performed preferentially in a stirred suspension system instead of a conventional packed bed. To facilitate the recovery and manipulation of nanoparticles, a promising method is to incorporate magnetism with the nanoparticles. Magnetic nanoparticles have great applications in the fields of high-density data storage, ferrofluids, magnetic resonance imaging, bioseparation, and biomedicine.[6–11,17,18] Numerous types of magnetic nanoparticles for various applications could be tailored by using functionalized natural or synthetic polymers to impart surface reactivity.[19–22] Accordingly, in this work, we develop a novel magnetic nano-adsorbent using Fe_3O_4 magnetic nanoparticles as the cores and polyacrylic acid (PAA) as the ionic exchange groups. The size, structure, and magnetic properties of the resultant magnetic nanoparticles and nano-adsorbents were characterized by transmission electron microscopy (TEM), X-ray diffraction (XRD), and the superconducting quantum interference device (SQUID) magnetometer. The binding of PAA to the magnetic nanoparticles *via* carbodiimide activation was confirmed by Fourier transform infrared (FTIR) spectroscopy, thermogravimetric analysis (TGA), differential thermal analysis (DTA) and X-ray photoelectron spectroscopy (XPS). In addition, the ion exchange capacity of the magnetic nano-adsorbent was determined, and its application to the separation of lysozyme from aqueous solution was also investigated.

Experimental

Polyacrylic acid solution (25%, degree of polymerization = 2000–3000) and sodium thiocyanate were purchased from Showa Chemical Co. (Tokyo). Crystallized and lyophilized lysozyme (EC 3.2.1.17) from hen's egg white (No. L-6876), *Micrococcus luteus* cells (ATCC, No.4698) and carbodiimide were supplied from Sigma Chemical Co. (St. Louis, MO). Bio-Rad reagent for protein assay was obtained from Bio-Rad Lab. (Hercules). Ferric chlorides, 6-hydrate was purchased from J. T. Baker (Phillipsburg). Glycine and natriumtetraborate-10-hydrate were obtained from Riedel-de Haën (Seelze). *o*-Phthaldialdehyde, β-mercaptoethanol and ferrous chloride tetrahydrate were purchased from Fluka (Buchs). Ammonium hydroxide (29.6%) was supplied by TEDIA (Fairfield). The water used throughout this work was the reagent-grade produced by a Milli-Q SP ultra-pure-water purification system from Nihon Millipore Ltd., Tokyo. All other chemicals were

 DOI: 10.1039/b207158d

guaranteed or analytical grade reagents commercially available and used without further purification.

Magnetic nanoparticles, Fe_3O_4, were prepared by co-precipitating Fe^{2+} and Fe^{3+} ions by ammonia solution and treating under hydrothermal conditions.[23,24] The ferric and ferrous chlorides (molar ratio 2 : 1) were dissolved in water at a concentration of 0.3 M iron ions. Chemical precipitation was achieved at 25 °C under vigorous stirring by adding NH_4OH solution (29.6%). During the reaction process, the pH was maintained at about 10. The precipitates were heated at 80 °C for 30 min, then washed several times with water and ethanol, and finally dried in a vacuum oven at 70 °C.

For the binding of PAA, 100 mg of magnetic nanoparticles were first added to 2 mL of buffer A (0.003 M phosphate, pH 6, 0.1 M NaCl). Then, the reaction mixture was sonicated for 10 min after adding 0.5 mL of carbodiimide solution (0.025g mL^{-1} in buffer A). Finally, 2.5 mL of PAA solution (6–60 mg mL^{-1} in buffer A) was added and the reaction mixture was sonicated for 30 min. The binding process was carried out at a constant temperature of 4 °C. The PAA-bound magnetic nanoparticles were recovered from the reaction mixture by placing the bottle on a permanent magnet with a surface magnetization of 6000 G. The magnetic particles settled within 1–2 min and then were washed with buffer A. It should be mentioned that NaCl was used for the flocculation of the magnetic nanoparticles.[25] Its addition could accelerate the magnetic separation, particularly in alkaline solutions.

TGA and DTA were done on the dried magnetic nanoparticles in air with a heating rate of 10 °C min^{-1} on Shimadzu TA-50WSI TGA and DTA instruments, respectively. By redispersing the magnetic nanoparticles in ethanol and depositing them on an aluminium oxide support by solvent evaporation at 80 °C, the obtained samples were used for XPS measurements on a Fison (VG) ESCA 210 spectrometer equipped with an Al Kα X-ray source (1486.6 eV photons). The XPS spectra were adjusted for offset due to the floodgun by fitting to the doublet Au 4f envelope (binding energy of 84.0 eV) as a reference.[26] The size and morphology of magnetic nanoparticles were observed by TEM using a JEOL Model JEM-1200EX at 80 kV. The sample for TEM analysis was obtained by placing a drop of the magnetic-nanoparticle-dispersed ethanol solution onto a Formvar-covered copper grid and evaporating in air at room temperature. Before withdrawing the sample, the dispersed solution was sonicated for 1 min to obtain a better particle dispersion on the copper grid. For each sample, over 60 particles from different parts of the grid were used to estimate the mean diameter of particles. XRD measurement was performed on a Rigaku D/max III.V X-ray diffractometer using Cu Kα radiation (λ = 0.1542 nm). Magnetic measurements were done using a SQUID magnetometer (MPMS7, Quantum Design). The amounts of PAA bound on the magnetic nanoparticles were estimated by the percentage weight losses from the corresponding TGA curves. The binding of PAA to the magnetic nanoparticles was checked using an FTIR spectrometer (Bio-Rad FTS 165). All the PAA-bound magnetic nanoparticles used for the analyses by TEM, XRD, XPS, SQUID, and FTIR contained a fixed PAA amount of 12 mg on 100 mg Fe_3O_4.

The amount of NH_2 groups on the surface of the magnetic nanoparticles was determined by spectrophotometric assay based on the reaction of o-phthaldialdehyde (OPA) and β-mercaptoethanol (BME) with the primary amines.[27] First, two reagents were freshly prepared as follows. For reaction of the primary amines of the solid, 300 μL ethanol solution containing 0.25 M OPA and 300 μL of 0.1 M sodium borate (pH 9.5) containing 4% β-mercaptoethanol were added to water to yield 50 mL of reagent 1 (R_1). For the determination of excess OPA, 500 μL of 0.06 M glycine and 500 μL of 0.1 M sodium borate (pH 9.5) containing 0.5% BME were added to water to yield 30 mL of reagent 2 (R_2). Secondly, 20 mg of magnetic nanoparticles were incubated with 5 mL reagent R_1 for 5 min at 25 °C. The liquid solution was then separated from the magnetic nanoparticles *via* a permanent magnet. To 4 mL of 0.1 M sodium borate and 200 μL of reagent R_2 in a test-tube, 100 μL of supernatant was added. After mixing by vortex for several minutes, the absorbance of the sample at 340 nm was determined on a Hitachi U-3000 spectrophotometer. Finally, a reference solution was prepared according to the above procedures but in the absence of the magnetic nanoparticles. The concentration of amino groups on the surface of the magnetic nanoparticles was determined from the difference between the absorbances of the reference solution and the sample, using the molar absorption coefficient ε = 6623 M^{-1} cm^{-1}.

The ion exchange capacity of the PAA-bound magnetic nanoparticles as adsorbents was determined as follows. First, 100 mg of magnetic nano-adsorbent was incubated in 5 mL of 1.0 M NaCl solution. The preliminary experiment revealed the adsorption process reached equilibrium after mixing by vortex for about 1 min, the magnetic nano-adsorbents were recovered magnetically after several minutes and then rinsed with water. Secondly, the magnetic nano-adsorbents were added to 5 mL of HNO_3 solution (pH 3) to release the Na^+ ions. After mixing by vortex for several minutes, the mixture was separated magnetically and the supernatant was used to determine the concentration of Na^+ ions by inductively coupled plasma atomic emission spectrometry (Jobin-Yvon PA Norama).

The adsorption of lysozyme on the magnetic nano-adsorbents was investigated in 0.1 M phosphate buffer (pH 2–8) at 25 °C. In general, 100 mg magnetic nano-adsorbent were added to 5 mL of lysozyme solution (4 mg mL^{-1}). After mixing by vortex for 1 min, the magnetic nano-adsorbents were removed magnetically from the lysozyme solution. The amount of lysozyme adsorbed on the magnetic nano-adsorbent was estimated from the concentration change of lysozyme in solution after adsorption by a colorimetric method at 595 nm using the Bio-Rad reagent for protein assay with bovine serum albumin as the standard. The desorption of lysozyme was studied by putting the removed magnetic nanoparticles into 0.1 M phosphate buffer (pH 5) containing 0.1–2 M NaSCN. After mixing for several minutes and removing the magnetic nano-adsorbents, the concentration of lysozyme in the liquid solution was measured to estimate the amount of lysozyme desorbed.

The activity of the lysozyme was determined by a turbidimetric assay procedure.[28] A suspension of 0.2 mg mL^{-1} *Micrococcus luteus* cells was prepared in 0.003 M phosphate (pH 6 and 25 °C). To 2.95 mL of the suspension, 0.05 mL of lysozyme solution (10 μg mL^{-1}) was added and mixed immediately. The activity of the lysozyme was defined as the initial linear decreasing rate of absorbance at 450 nm on a Hitachi U-3000 spectrophotometer. The absorbance at 450 nm was recorded every 5 s for 2 min, and the decreasing rate was estimated by linear regression.

Results and discussion

The TGA and DTA curves for naked and PAA-bound Fe_3O_4 magnetic nanoparticles are shown in Fig. 1. For naked Fe_3O_4, no significant peak appeared in the DTA curve. Also, the TGA curve shows that the weight loss over the temperature range from 100 to 400 °C was only about 2%. This might be due to the loss of residual water and the amine groups (shown later) in the sample. On the other hand, for PAA-bound Fe_3O_4, the TGA curve shows two weight loss steps. The first weight loss step over the temperature range from 100 to 250 °C might be due to the loss of residual water in the sample. The sharp weight loss around 260 °C was due to the burning of PAA. There was no

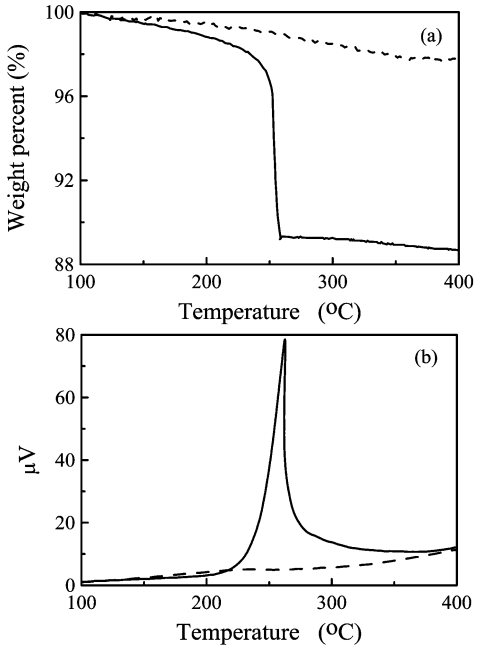

Fig. 1 Thermogravimetric (a) and differential thermal (b) analyses of magnetic nanoparticles without (——) and with (—) bound PAA.

significant weight change from 260 to 400 °C, implying the presence of only iron oxide within the temperature range. The thermochemical behavior described above by the TGA curve was consistent with that indicated by the DTA curve. The main exothermic peak at 263 °C could be attributed to the burning of PAA. Accordingly, it revealed that PAA indeed could be bound to Fe_3O_4 magnetic nanoparticles.

From the percentage weight loss in the TGA curve, the amount of PAA bound on the magnetic nanoparticles was estimated. The experiment was performed in 5 mL of PAA solution containing a constant Fe_3O_4 amount of 100 mg. As shown in Fig. 2, with increasing amounts of PAA in solution, the amount of PAA bound on the magnetic nanoparticles increased first and then remained at 12 mg when the amount of PAA in solution was above 100 mg. Thus, the maximum weight ratio of PAA bound to Fe_3O_4 nanoparticles could be determined to be 0.12. In addition, the density of Fe_3O_4 is 5.18 g cm^{-3} and the average molecular weight of PAA was about 180,000. Assuming the resultant Fe_3O_4 nanoparticles were spherical, it could be estimated that on average two PAA molecules were bound to one Fe_3O_4 particle when the weight ratio of PAA to Fe_3O_4 was 0.12. Thus, the binding of PAA to Fe_3O_4 nanoparticles in this work has been achieved at a molecular level.

To realize the binding mechanism, the FTIR spectra of naked Fe_3O_4, PAA and PAA-bound Fe_3O_4 were examined as

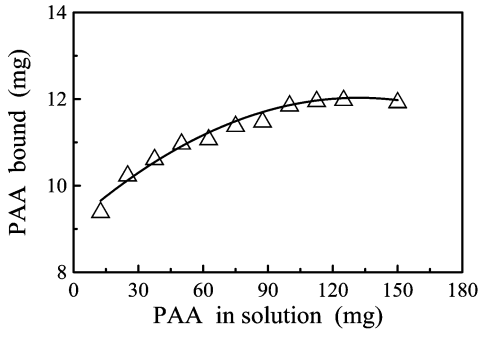

Fig. 2 Effect of the amount of PAA in solution on the amount of PAA bound on the magnetic nanoparticles.

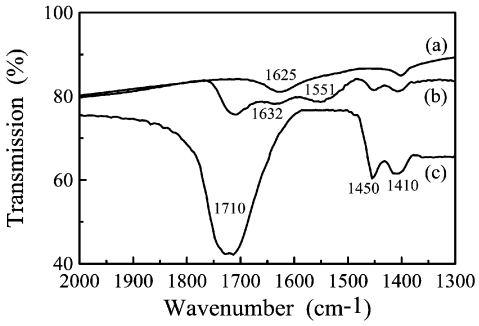

Fig. 3 FTIR spectra of the magnetic nanoparticles without (a) and with (b) bound PAA and (c) pure PAA. PAA : Fe_3O_4 = 3 : 25 w/w.

shown in Fig. 3. The peak around 1410 cm^{-1} observed in each of the three cases relates to the –OH group. For naked Fe_3O_4 and PAA, the peak at 1710 cm^{-1} relates to the carbonyl (C=O) group and the peak at 1450 cm^{-1} relates to the $–CH_3$ and $–CH_2–$ groups, confirming the binding of PAA on Fe_3O_4. From naked and PAA-bound Fe_3O_4, the characteristic band of $–NH_2$ at 1625 cm^{-1} disappeared and bands characteristic of $RCONR_2$ at 1632 and 1551 cm^{-1} appeared after binding PAA, implying the binding was accomplished by a reaction between the amino groups on the Fe_3O_4 nanoparticles and the carbonyl group of the PAA with carbodiimide activation. As for the amine group, it might be formed due to the use of concentrated ammonia solution during the co-precipitation of Fe^{2+} and Fe^{3+} ions.

The amount of amino groups on the Fe_3O_4 nanoparticles were also quantified by a spectrophotometric assay based on the reaction of the amino groups of the solids with an excess of OPA and the subsequent quantitative determination of the unreacted OPA by reaction with glycine. It was found that about 351 amino groups were available on a naked Fe_3O_4 nanoparticle while no amino groups were detected on PAA-bound Fe_3O_4 nanoparticles. This result was consistent with that obtained from FTIR analysis.

In addition, the XPS spectra of C 1s and N 1s for the naked and PAA-bound Fe_3O_4 nanoparticles were also measured to study the covalent binding of PAA onto the Fe_3O_4 nanoparticles. From the XPS spectra of C 1s in Fig. 4, it was observed that peptide chains were formed after PAA binding according to the –C=O–NH– feature at 288.4 eV and the C–N feature at 286.5 eV.[26] Fig. 5 shows the XPS spectra of N 1s. After PAA binding, the binding energy of the –NH– feature increased from 400.3 to 401.6 eV. The increased binding energy reflected the decreased electron density on the N atom and might result from binding between N and C atoms.[29,30] The

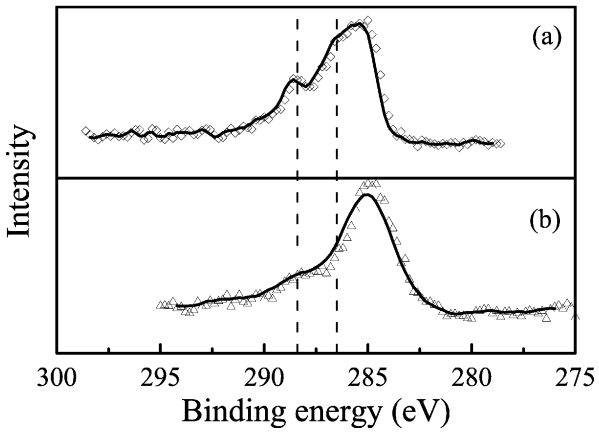

Fig. 4 XPS spectra of C 1s for the magnetic nanoparticles with (a) and without (b) bound PAA. PAA : Fe_3O_4 = 3 : 25 w/w.

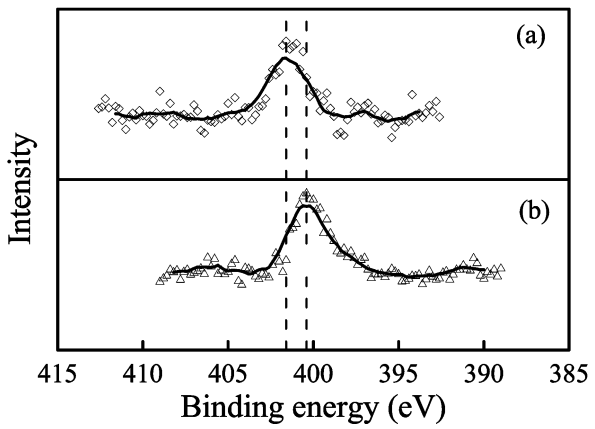

Fig. 5 XPS spectra of N 1s for the magnetic nanoparticles with (a) and without (b) bound PAA. PAA : Fe_3O_4 = 3 : 25 w/w.

main features at about 285 eV relate to saturated hydrocarbons, which might be due to the presence of ethanol, which had adsorbed onto the Fe_3O_4 during the washing process. According to the above, it can be seen that the binding of PAA onto the Fe_3O_4 nanoparticles was accomplished *via* a reaction between the amino and carboxyl groups.

Typical TEM micrographs for the magnetic nanoparticles with and without bound PAA are shown in Fig. 6. It was clear that the naked Fe_3O_4 particles were essentially very fine and monodisperse with a mean diameter of 13.2 nm. After binding PAA, the particles remained discrete and had a similar mean diameter. This reveals that the binding process did not significantly result in agglomeration or a change in size of the particles. This could be attributed to the fact that the reaction occurred only on the particle surface and, as stated above, on average only two PAA molecules were bound to a particle.

Fig. 7 shows the XRD patterns for the magnetic nanoparticles without and with bound PAA. Six characteristic peaks for Fe_3O_4 (2θ = 30.1, 35.5, 43.1, 53.4, 57.0 and 62.6°), marked by their indices ((220), (311), (400), (422), (511) and (440)), were observed for both samples. These peaks are in agreement with those in JCPDS file (PCPDFWIN v.2.02, PDF No. 85-1436) and reveal that the resultant particles were pure Fe_3O_4 with a spinel structure. Also, the binding process did not result in a phase change for the Fe_3O_4.

The plots of magnetization *versus* magnetic field (*M–H* loop) at 25 °C for typical magnetic nanoparticles without and with

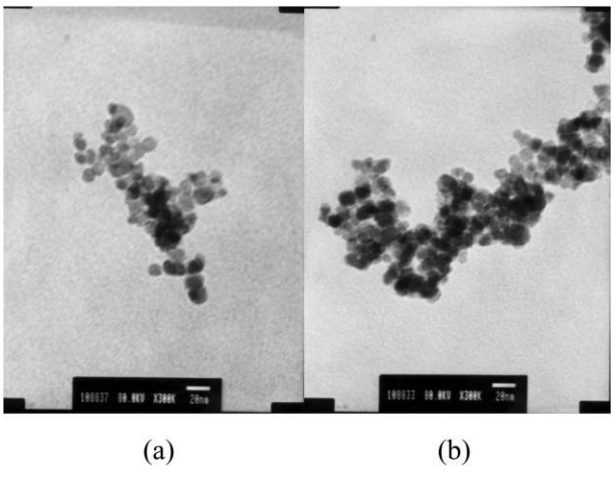

Fig. 6 Transmission electron micrographs of magnetic nanoparticles without (a) and with (b) bound PAA. PAA : Fe_3O_4 = 3 : 25 w/w.

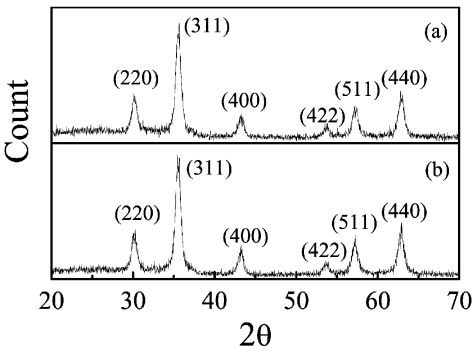

Fig. 7 XRD patterns of magnetic nanoparticles with (a) and without (b) bound PAA. PAA : Fe_3O_4 = 3 : 25 w/w.

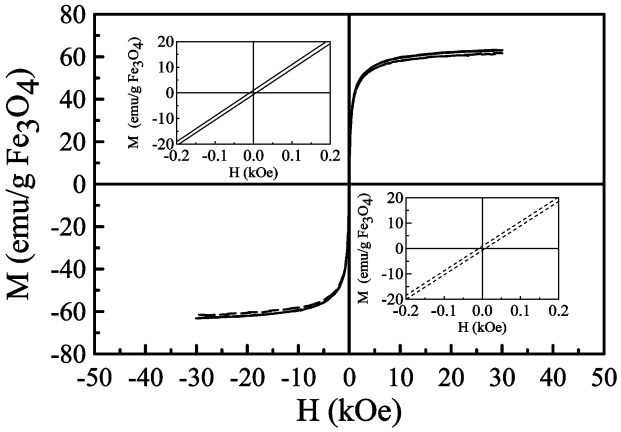

Fig. 8 Magnetization *vs.* magnetic field for the magnetic nanoparticles without (—) and with (——) bound PAA at 25 °C. PAA : Fe_3O_4 = 3 : 25 w/w.

bound PAA are illustrated in Fig. 8. The very weak hysteresis revealed the resultant magnetic nanoparticles were superparamagnetic. From the plots of *M vs. H* and their enlargements near the origin, as shown in the insets in Fig. 8, the saturation magnetization (M_s), remanent magnetization (M_r), coercivity (H_c), and squareness ($S_r = M_r/M_s$) were determined to be 63.2 emu g^{-1}, 0.83 emu g^{-1}, 8.3 Oe, and 0.013, respectively, for naked magnetic nanoparticles, and 61.7 emu g^{-1}, 0.82 emu g^{-1}, 8.5 Oe, and 0.013, respectively, for PAA-bound magnetic nanoparticles.

The saturation magnetization of Fe_3O_4 nanoparticles was reduced to 69% of the bulk Fe_3O_4 (92 emu g^{-131}). The reduction in M_s might be due to the decrease in particle size and the accompanied increase in surface area. It is known that the energy of a magnetic particle in an external field is proportional to its size *via* the number of magnetic molecules in a single magnetic domain. When this energy becomes comparable to the thermal energy, thermal fluctuations will significantly reduce the total magnetic moment at a given field.[32] It is also known that the magnetic molecules on the surface lack complete coordination and the spins are likewise disordered.[33] This phenomenon is more significant for the nanoparticles due to their large surface-to-volume ratio. So, the smaller M_s value for the nanoparticles compared with the corresponding bulk materials is reasonable. In addition, the disordered structure in the amorphous materials and at the interface, such as that found at a grain boundary, has been shown to cause a decrease in the effective magnetic moment.[34] Therefore, another possible reason for the diminution in M_s might be the incomplete crystallization of the Fe_3O_4 nanoparticles, which led to amorphous impurities undetectable by XRD. Finally, electron

exchange between the ligand and the surface atoms could also quench the magnetic moment.[35] Therefore, the amino groups on Fe_3O_4, as observed above, might be another reason for the decrease in the M_s value.

The M_s value for the PAA-bound magnetic nanoparticles was slightly lower than that for the naked ones. This might result from the binding of PAA on the particle surface, which might quench the magnetic moment. However, the reduction in M_s due to PAA binding was only 2.4%. This might be due to the fact that only two PAA molecules were bound to a Fe_3O_4 nanoparticle. The M_r, H_c, and S_r values were so small that they were superparamagnetic and implied that the thermal energy required to demagnetize became dominant over spontaneous magnetization. After PAA binding, these values did not change significantly. The differences were within limits and further discussion is unnecessary.

The feasibility of PAA-bound magnetic nanoparticles as magnetic nano-adsorbents was investigated in 1.0 M NaCl solution. It was found that the ionic exchange capacity of PAA-bound magnetic nanoparticles was 1.64 mequiv g^{-1}, much higher than those of commercial ionic exchange resins (usually <0.1 mequiv g^{-1}). Preliminary experiments revealed that the ionic exchange capacity of the naked magnetic nanoparticles for the adsorption of Na^+ ions was negligible (<0.02 mequiv g^{-1}) compared with that of PAA-bound ones. This revealed that the ionic exchange capacity of the PAA-bound magnetic nanoparticles was attributable to the presence of the PAA molecules. According to the amount of PAA bound and the degree of polymerization of the PAA (2000–3000), the theoretical ionic exchange capacity of PAA-bound magnetic nano-adsorbents could be estimated to be 1.38–1.67 mequiv g^{-1}, in agreement with the empirical value. Thus, the resultant PAA-bound magnetic nanoparticles could indeed be used as magnetic nano-adsorbents.

Since they have no internal pores, the novel magnetic nano-adsorbents might be useful for the adsorption of large solutes such as proteins. A test for the adsorption of lysozyme by magnetic nano-adsorbent was conducted in 0.1 M phosphate buffer (pH 2–8) at a lysozyme concentration of 4 mg mL^{-1} at 25 °C. It was found that lysozyme could be completely adsorbed within 1 min at pH 3–5. The maximum amount of lysozyme adsorbed on the magnetic nano-adsorbents was about 0.22 mg mg^{-1}, obviously higher (3-fold) than that using other magnetic and nonmagnetic affinity supports.[20,36] The desorption of lysozyme was investigated at 25 °C in 0.1 M phosphate buffer (pH 5) containing 0.1–2 M NaSCN. It was found that the lysozyme could be completely desorbed within 1 min when the NaSCN concentration was above 1.0 M. The adsorption/desorption tests revealed the resultant magnetic nano-adsorbents were quite efficient adsorbents. Also, the adsorption and desorption rates were very fast because of the absence of internal diffusion resistance.

In addition, the effect of adsorption/desorption on the activity of the lysozyme was examined. The initial activity of the lysozyme before adsorption was 0.0095 min^{-1}, it was found that the lysozyme retained about 95% activity (0.0090 min^{-1}) after adsorption/desorption. This revealed the adsorption/desorption did not result in a significant reduction of enzyme activity.

Accordingly, the resultant nano-adsorbents can not only be manipulated magnetically but also exhibit a quite high adsorption capacity and fast adsorption rate due to their high specific surface area and the absence of internal diffusion resistance. Although their capacity was slightly lower than those of some natural and synthetic zeolites,[37] the novel magnetic nano-adsorbents were useful for the separation of large solutes, particularly biomolecules such as enzymes, proteins, and DNA.

Conclusions

A novel magnetic nano-adsorbent was prepared by covalently binding PAA on Fe_3O_4 magnetic nanoparticles. The maximum weight ratio of PAA to Fe_3O_4 was 0.12 (*i.e.*, on average two PAA molecules bound to one magnetic nanoparticle). FTIR, XPS and thermal analyses suggested that the binding of PAA on the magnetic nanoparticles was accomplished by reaction between the amino groups on the Fe_3O_4 nanoparticles and the carbonyl group of the PAA with carbodiimide activation. Characterization by TEM, XRD and SQUID magnetometer indicated the formation of pure Fe_3O_4 superparamagnetic nanoparticles and the binding process did not significantly affect the size, structure, and magnetic properties. In addition, the resultant PAA-bound magnetic nanoparticles had an ionic exchange capacity of 1.64 mequiv g^{-1}, much higher than those of commercial ion exchange resins. Lysozyme was adsorbed and desorbed efficiently and quickly (within 1 min) due to the high adsorption capacity and the absence of any internal diffusion resistance. Also, the lysozyme retained 95% activity after adsorption/desorption. The novel magnetic nanoparticles developed in this work indeed possessed quite low mass transfer resistance and a high ionic exchange capacity, particularly for large solutes. This work should be helpful for the development of adsorbents and adsorption processes.

Acknowledgement

This work was performed under the auspices of the National Science Council of the Republic of China, to which the authors wish to express their thanks.

References

1 C. N. R. Rao and A. K. Cheetham, *J. Mater. Chem.*, 2001, **11**, 2887.
2 S. Chen and N. Li, *J. Mater. Chem.*, 2002, **12**, 1124.
3 P. Audebert, S. Sadki, F. Miomandre, G. Lanneau, R. Frantz and J. O. Durand, *J. Mater. Chem.*, 2002, **12**, 1099.
4 S. Nuβ, H. Böttcher, H. Wurm and M. L. Hallensleben, *Angew. Chem. Int. Ed.*, 2001, **40**, 4016.
5 C. Mangeney, F. Ferrage, I. Aujard, V. Marchi-Artzner, L. Jullien, O. Ouari, E. D. Rékaï, A. Laschewsky, I. Vikholm and J. W. Sadowski, *J. Am. Chem. Soc.*, 2002, **124**, 5811.
6 Y. Sahoo, H. Pizem, T. Fried, D. Golodnitsky, L. Burstein, C. N. Sukenik and G. Markovich, *Langmuir*, 2001, **17**, 7907.
7 Y. Lu, Y. Yin, B. T. Mayers and Y. Xia, *Nano Lett.*, 2002, **2**, 183.
8 A. Millan and F. Palacio, *Appl. Organomet. Chem.*, 2001, **15**, 396.
9 S. Mornet, A. Vekris, J. Bonnet, E. Duguet, F. Grasset, J. H. Choy and J. Portier, *Mater. Lett.*, 2000, **42**, 183.
10 Y. Zhang, N. Kohler and M. Zhang, *Biomaterials*, 2002, **23**, 1553.
11 L. Suber, S. Foglia, G. M. Ingo and N. Boukos, *Appl. Organomet. Chem.*, 2001, **15**, 414.
12 F. Caruso, *Adv. Mater.*, 2001, **13**, 11.
13 C. Sanchez, G. J. de A. A Soler-Illia, F. Ribot, T. Lalot, C. R. Mayer and V. Cabuil, *Chem. Mater.*, 2001, **13**, 3061.
14 N. Shipway and I. Willner, *Chem. Commun.*, 2001, **20**, 2035.
15 S. Förster and T. Plantenberg, *Angew. Chem. Int. Ed.*, 2002, **41**, 688.
16 M. Niemeyer, *Angew. Chem. Int. Ed.*, 2001, **40**, 4128.
17 W. Schütt, C. Grüttner, U. Häfeli, M. Zborowski, J. Teller, H. Putzar and C. Schümichen, *Hybridoma*, 1997, **16**, 109.
18 I. Šafařík and M. Šafaříková, *J. Chromatogr., B*, 1999, **722**, 33.
19 R. Pieters, R. A. Williams and C. Webb, in *Colloid and Surface Engineering: Applications in the Process Industries*, ed. R. A. Williams, Butterworth-Heinemann, Oxford, 1992, pp. 248–333.
20 X. D. Tong, B. Xue and Y. Sun, *Biotechnol. Prog.*, 2001, **17**, 134.
21 H. P. King, D. Cunliffe, S. Davies, N. A. Turner and E. N. Vulfson, *Biotechnol. Bioeng.*, 1998, **60**, 419.
22 B. Xue and Y. Sun, *J. Chromatogr., A*, 2002, **947**, 185.
23 M. H. Liao and D. H. Chen, *Biotechnol. Lett.*, 2001, **23**, 1723.
24 H. Chen and M. H. Liao, *J. Mol. Catal. B*, 2002, **16**, 283.
25 A. Kondo and H. Fukuda, *J. Ferment. Bioeng.*, 1997, **84**, 337.

26 L. Jiang, A. Glidle, A. Griffith, C. J. McNeil and J. M. Cooper, *Bioelectrochem. Bioenerg.*, 1997, **42**, 15.
27 V. G. Janolino and H. E. Swaisgood, *Appl. Biochem. Biotechnol.*, 1992, **36**, 81.
28 E. Ruckenstein and X. Zeng, *Biotechnol. Bioeng.*, 1997, **56**, 610.
29 R. W. Murray, *Acc. Chem. Res.*, 1980, **13**, 135.
30 L. Xu, M. Li and E. Wang, *Mater. Lett.*, 2002, **54**, 303.
31 V. Zaitsev, D. S. Filimonov, I. A. Presnyakov, R. J. Gambino and B. Chu, *J. Colloid Interface Sci.*, 1999, **212**, 49.
32 K. V. P. M. Shafi, A. Gedanken, R. Prozorov and J. Balogh, *Chem. Mater.*, 1998, **10**, 3445.
33 D. H. Chen and S. H. Wu, *Chem. Mater.*, 2000, **12**, 1354.
34 J. H. Hwang, V. P. Dravid, M. H. Teng, J. J. Host, B. R. Elliott, D. L. Johnson and T. O. Mason, *J. Mater. Res.*, 1997, **12**, 1076.
35 D. A. Vanleeuwen, J. M. Vanruitenbeek, L. J. Dejongh, A. Ceriotti, G. Pacchioni, O. D. Häberlen and N. Rösch, *Phys. Rev. Lett.*, 1994, **73**, 1432.
36 S. Şenel, S. Akgöl, Y. Arica and A. Denizli, *Polym. Int.*, 2001, **50**, 143.
37 E. Harland, *Ion Exchange: Theory and Practice*, The Royal Society of Chemistry, Cambridge, 1994.